Bulg. J. Phys. **40** (2013) 307–324

p- or n-Doping Effects on the Phonon Spectrum of Single- and Bi-Layer Graphene

A.T. Apostolov[1], **I.N. Apostolova**[2], **J.M. Wesselinowa**[3]

[1]University of Architecture, Civil Engineering and Geodesy, Faculty of Hydrotechnics, 1 Hr. Smirnenski Blvd., 1046 Sofia, Bulgaria
[2]University of Forestry, Faculty of Forest Industry, 10 Kl. Ohridsky Blvd., 1756 Sofia, Bulgaria
[3]University of Sofia, Faculty of Physics, 5 J. Bouchier Blvd., 1164 Sofia, Bulgaria

Abstract. Using a microscopic model and the Green's function technique we have studied the phonon properties of ion doped single- and bilayer graphene. There are differences in the behavior of the energy and damping of the G and 2D modes in a p- and n-doped single-layer graphene. A microscopic explanation is proposed. The influence of the electron-phonon interaction is discussed. We report also phonon energy and damping renormalization in bi-layer graphene as a function of doping. The results are in qualitative agreement with the experimental data.

PACS codes: 63.22.Rc; 68.65.Pq; 61.72.Bb; 63.20.kd; 63.20.kg

1 Introduction

Doping is the most feasible method to control the properties in graphene. The B and N atoms are the natural candidates for doping in graphene because of their similar atomic size as that of C and of their hole acceptor and electron donor characters for substitutional B- and N-doping, respectively [1-5]. The substitutional doping is also a useful method to open band gap of graphene as proved by the theoretical work about B-, N- and Bi-doping in graphene [6-8]. Transition metal (TM) adatoms and clusters on graphene have recently been also a topic of great interest: at low density, they are expected to induce doping, scattering, and novel magnetic and superconducting behavior; at high density (up to continuous coverage), they may locally dope or modify the band structure of graphene. The electronic and magnetic properties of graphene doped with different TM ions are investigated experimentally, for example with Ni [9], Mn [10], Fe [11,12] and theoretically used a quantum Monte Carlo method [13] and

phenomenological analysis [14,15]. Through first-principles density functional theory (DFT) and ab initio calculations, the effect of substitutional doping on the structure of graphene as well as on the electronic and magnetic properties was studied [10,16-20]. Pedersen and Pedersen [21] have analyzed B and N substitutional impurities in graphene using a self-consistent tight-binding approach and determined the local density of states at the impurity site and, thereby, identify acceptor and donor energy resonances.

Raman spectroscopy is a fast and nondestructive means to characterize graphene samples. In particular, the Raman spectra are strongly affected by doping. Unfortunately there are not so many theoretical studies about the doping effects on the phonon properties in graphene. While the resulting change in position and width of the G peak can be explained by the nonadiabatic Kohn anomaly at Γ, the significant doping dependence of the 2D peak intensity has not been understood yet. A detailed analysis of the dependence of the Raman intensity of graphene on doping and disorder is presented in [22]. The Raman scattering process in graphene is always resonant, i.e. involves real electronic states, and this affects the Raman intensity. Thus, the analysis of the Raman intensity of graphene can provide useful information on the Raman scattering process itself, in particular on the interaction between the fundamental excitations in graphene, such as electron-phonon and electron-defect interactions. While the intensity of the G peak is not strongly affected by small amount of doping or disorder, the intensity of the 2D peak strongly decreases with increasing doping or disorder [22]. Recently, the electronic and phonon band structures of pristine few layer and Al or Ag doped graphene are studied by Gupta et al. [23] using first principles calculations. Based on the density functional theory Sahin et al. [24] have studied the interaction of chlorine atoms with graphene predicting the existence of possible chlorinated graphene derivatives. They reported that the phonon frequencies are lowered due to the saturation of C atoms with heavy Cl atoms. The electron-electron interactions and doping dependence of the two-phonon Raman intensity in graphene are investigated by Basko et al. [25]. The optical reflectivity and Raman scattering in few-layer-thick graphene highly doped by K and Rb is reported by Jung et al. [26]. The Raman G mode is downshifted and significantly broadened. Graphene phonons are measured as a function of electron doping via the addition of potassium adatoms [27]. In the low doping regime, the in-plane carbon G peak hardens and narrows with increasing doping, whereas at high doping the G peak strongly softens and broadens. Abdula et al. [28] have examined how doping and defects alter linewidths and lifetimes of G-band optical phonons in carbon nanotubes. It suggests that by N doping of graphene the structural tension and strain of graphene cause the more prominent spectra upshift [3-5]. Choudhury et al. have pointed out that there are differences between the charge-transfer doping and electrochemical doping [29].

In our previous papers we have studied the temperature, size [30] and substrate [31] effects on the G and 2D phonon mode behavior in graphene. The aim of the

present paper is using a microscopic model and the Green's function method to investigate the ion doping dependence of the phonon energies and damping of the G and 2D modes in single- (SLG) and bi-layer (BLG) graphene.

2 Model

We are interested on doping defects in graphene, i.e. in a given lattice site the C atom is chemical replaced for example by B, N, Al, S. This leads to changes of the electron and phonon properties in graphene. The doping ions lead to the following effects: (i) they act as doping scattering centers; (ii) they act as donors for electrons (N) or holes (B); (iii) they cause lattice distortion. In the case of B-doping the absolute value of the hopping integral increases in comparison to the C-C binding value ($r_B = 0.85$ Å whereas $r_C = 0.7$ Å). By N doping ($r_N = 0.65$ Å) the hopping integral is reduced. We assume that the local energy of a C atom on a given site in a pure (an undoped) lattice is zero. Therefore the smaller atom number of B would lead to positive local energy on a given site in the graphene matrix, whereas for B this energy would be negative. The ion doping causes also changes of the lattice modes in the following ways: (i) the so-called isotope effect, which is due to the mass difference between doping and C atoms; (ii) changes in the values of the force constants.

Taking into account these basic assumptions the Hamiltonian for a multilayer chemical doped graphene can be written as

$$H = H_0 + H^{\text{imp}}. \tag{1}$$

Here H_0 is the Hamiltonian of the pure graphene including the lattice anharmonism and the electron-phonon interaction and is defined in our previous paper [30] and H^{imp} describes the doping contribution

$$H^{\text{imp}} = H^{\text{imp}}_{\text{el}} + H^{\text{imp}}_{\text{ph}}. \tag{2}$$

We denote the numbers of doping ions and of C atoms with n_i and N_c, respectively. We consider the case of small doping, i.e. $n_i \ll N_c$. We neglect the interaction between the doping ions.

$$H^{\text{imp}}_{\text{el}} = H^{\text{imp}}_{\text{pot}} + H^{\text{imp}}_{\text{int}}. \tag{3}$$

The first term $H^{\text{imp}}_{\text{pot}}$ gives the contribution in the local potential energy of the p-lattice site in the n-layer of graphene (we assume that the defects are situated only on A-sites)

$$H^{\text{imp}}_{\text{pot}} = \sum_{pn\sigma}^{n_i} V_p a^+_{pn\sigma} a_{pn\sigma}. \tag{4}$$

The second term in Eq. (3) $H_{\rm int}^{\rm imp}$ describes the changes of the hopping integrals between the first and second neighbors of a given doping ion

$$H_{\rm int}^{\rm imp} = \sum_{pjnl\sigma\sigma'}^{n_i N} t_{pjnl}^{\rm imp}(eff)(a_{pn\sigma}^{+} b_{jl\sigma} + b_{jl\sigma}^{+} a_{pn\sigma}) + \sum_{pjnl\sigma\sigma'}^{n_i N} t_{pjnl}^{\prime \rm imp} a_{pn\sigma}^{+} a_{jl\sigma} \quad (5)$$

with

$$t_{pjnl}^{\rm imp}(eff) = t_{pjnl}^{\rm imp} + \frac{1}{2}\sum_{r}^{n} g_{1pjr}^{\rm imp}\langle Q_r\rangle + \frac{1}{4}\sum_{rs}^{n} g_{2pjrs}^{\rm imp}\langle Q_r Q_s\rangle. \quad (6)$$

The operators a and b refer to the A and B sites inside of the graphene Bravais lattice unit cell [30]. $g_1^{\rm imp}$ and $g_2^{\rm imp}$ determine the doping contributions to the electron-phonon interaction. We combine the effects of local changes in the atom energy with the amplitude of the hopping integral.

In the doped graphene the Fermi level is removed which causes changes of the equilibrium lattice parameter. This leads to hardening or softening of the phonon modes and to changes of the phonon dispersion. For the phonon system is the contribution to the energy of the doped p-site

$$H_{ph}^{\rm imp} = \sum_{pj}^{n_i} (\Phi_{pj}^{\rm imp}(0) + \Phi_{pj}^{\rm imp}(1)) Q_p Q_j. \quad (7)$$

Here $\Phi_{pj}^{\rm imp}(0) = \omega_{p0}\omega_{j0}(1+\Delta m)$ with $\Delta m = (M^0 - M^{\rm imp})/M^0$ describes the influence of the isotopic effect on the phonon properties in the doted graphene which is connected usually with the appearing of local phonon modes. $\Phi_{pj}^{\rm imp}(1)$ gives the renormalization of the phonon spectrum due to the changes of the anharmonic force constants and especially due to the electron-phonon interaction in a given layer

$$\Phi_{pj}^{\rm imp}(1) = -\frac{1}{3!}\sum_{r}^{n} B_{pjr}^{\rm imp}\langle Q_r\rangle - \frac{1}{4!}\sum_{rs}^{n} A_{pjrs}^{\rm imp}\langle Q_r Q_s\rangle + \frac{1}{4}\sum_{r}^{n} g_{2pjr}^{\rm imp}\bar{n}_r^{ab\,\rm imp}. \quad (8)$$

$B^{\rm imp}$ and $A^{\rm imp}$ determine the doping contributions to the anharmonic terms. Between the layers we assume an ordering from type ABABAB.

Figure 1 demonstrates our model, i.e. a schematic geometry of doped graphene. There are given the vectors and the doping modulation of the hopping integrals between the first and second neighbors.

From theoretical point of view the ion doping leads to breaking of the translation invariance. Therefore we look for an approximation method to can work in the favored reciprocal lattice. We use the scattering matrix for determination of the one-particle Green's function of the doped system on the basis of the Green's function of the pure crystal. Following this method one can write

$$G^{\rm imp} = G^0 + G^0 T G^{\rm imp}, \quad (9)$$

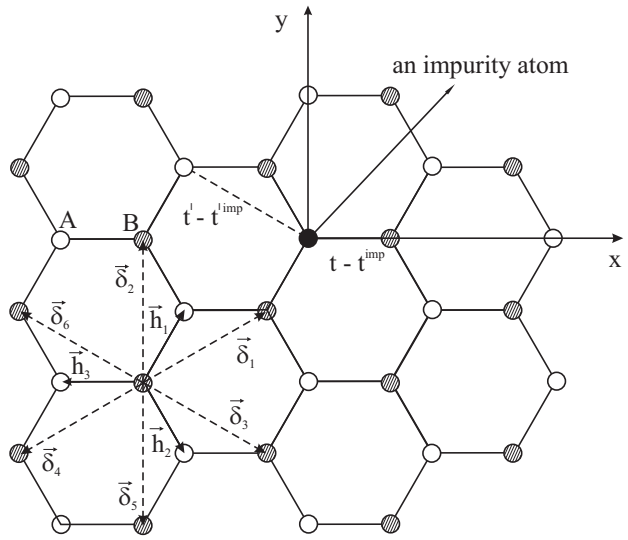

Figure 1. The carbon lattice where a host atom is replaced by an impurity one.

where T is the scattering matrix defined as

$$T = \frac{V}{1 - VG^0}. \tag{10}$$

V is the perturbation of the interactions and the local potential energies of the doped crystal. We assume firstly that in the matrix we have only one impurity and determine the so-called single-site scattering matrix, denoted with τ. By low impurity concentration ($x = n_i/N$) the Green's function for one impurity can be written as

$$G^{\text{imp}}_{\text{sng}} = G^0 + G^0 \tau G^0. \tag{11}$$

For concentration x we have: $T = Nx\tau$. Then for the Green's function for the doped crystal we obtain

$$G^{\text{imp}} = ((G^0)^{-1} - T)^{-1}. \tag{12}$$

Here we have neglected the interactions between the impurities.

3 Phonon Green's Function

The phonon Green's function in the pure graphene $G^0_{\text{ph}}(\mathbf{k}, \omega)$ is already calculated in our previous papers [30,31]. Now we will obtain the impurity phonon Green's function $G^{\text{imp}}_{\text{ph}}(\mathbf{k}, \mathbf{k}', \omega)$. After configuration averaging on all impurities the translational invariance is recovered:

$$\langle G^{\text{imp}}_{\text{ph}}(\mathbf{k}, \mathbf{k}', \omega) \rangle = G^{\text{imp}}_{\text{ph}}(\mathbf{k}, \omega) \delta_{\mathbf{k},\mathbf{k}'} \tag{13}$$

with

$$G_{\rm ph}^{\rm imp}(\mathbf{k},\omega) = \frac{1}{\omega^2 - (\omega_{\mathbf{k}}^0)^2 - \Sigma(\mathbf{k},\omega)}. \tag{14}$$

Here $\omega_{\mathbf{k}}^0$ is the phonon energy in the pure crystal, whereas $\Sigma(\mathbf{k},\omega)$ is the contribution from the doping. Following Davies and Langer [32], by small concentrations is $\Sigma(\mathbf{k},\omega)$ proportional to the scattering amplitude of a phonon or phonons from an isolated impurity:

$$\Sigma(\mathbf{k},\omega) = Nx\tau(\mathbf{k},\mathbf{k},\omega), \tag{15}$$

where

$$\begin{aligned}\tau(\mathbf{k},\mathbf{k}',\omega) &= \frac{\Phi_{k,k'}^{\rm imp}}{N} - \frac{1}{N}\sum_{k''}\Phi_{k,k''}^{\rm imp} G_{\rm ph}^{\rm imp}(\mathbf{k}'',\omega)\tau(\mathbf{k}'',\mathbf{k}',\omega) \\ &= \frac{1}{N}\frac{\Phi_{k,k'}^{\rm imp}}{1 + \frac{1}{N}\sum_{k''}\frac{\Phi_{k,k''}^{\rm imp}}{\omega^2 - (\omega_{k''}^0)^2 - \Sigma(\mathbf{k}'',\omega)}}. \end{aligned} \tag{16}$$

From Eq. (15), we obtain

$$\Sigma(\mathbf{k},\omega) = \frac{x\Phi_{k,k}^{\rm imp}}{1 + \frac{1}{N}\sum_{k''}\frac{\Phi_{k,k''}^{\rm imp}}{\omega^2 - (\omega_{k''}^0)^2 - \Sigma(\mathbf{k}'',\omega)}}. \tag{17}$$

After iteration of the process we can find the doping contribution to the phonon energy. Following the above described scattering matrix method in the denominator must stay the Green's function of the pure graphene, i.e. we have:

$$\Sigma(\mathbf{k},\omega) = \frac{x\Phi_{k,k}^{\rm imp}}{1 + \frac{1}{N}\sum_{k''}\frac{\Phi_{k,k''}^{\rm imp}}{\omega^2 - (\omega_{k''}^0)^2}}. \tag{18}$$

Finally we observe for the phonon energy of the doped graphene:

$$\Omega(\mathbf{k},\omega) = \pm\sqrt{(\omega_{\mathbf{k}}^0)^2 - \Sigma(\mathbf{k},\omega)}. \tag{19}$$

This is a formal solution and must be obtained from the poles of the Green's function $G_{\rm ph}^{\rm imp}(\mathbf{k},\omega)$. $\Phi_{k,k'}^{\rm imp}$ can be determined from

$$\begin{aligned}\Phi_{k,k'}^{\rm imp} &= (\omega_k^0)^2(1+\Delta m)\delta_{k,k'} - \frac{1}{3!}\sum_{k''}^{n}\omega_k^0 B_{k,k',k''}^{\rm imp}\langle Q_{k''}\rangle \\ &- \frac{1}{4!}\sum_{k'',k'''}^{n}\omega_k^0 A_{k,k',k'',k'''}^{\rm imp}\langle Q_{k''}Q_{k'''}\rangle + \frac{1}{4}\sum_{k''}^{n}\omega_k^0 g_{2k,k',k''}^{\rm imp}\bar{n}_{k''}^{ab\,\rm imp}. \end{aligned} \tag{20}$$

We make in $\Phi^{\text{imp}}_{k,k'}$, in the sum in Eq. (20) the following approximation, i.e. $\Phi^{\text{imp}}_{k,k'} \approx (\omega^0_k)^2(1+\Delta m)\delta_{k,k'}$. Finally we observe for $G^{\text{imp}}_{\text{ph}}(\mathbf{k},\omega)$:

$$G^{\text{imp}}_{\text{ph}}(\mathbf{k},\omega) = \frac{1}{\omega^2 + (1+\Delta m)(\omega^0_k)^2 - x\Phi^{\text{imp}}_{k,k}}. \tag{21}$$

From here the phonon energy of the doped grapheme is obtained as:

$$\omega^{\text{imp}}_{\mathbf{k}} = \pm\sqrt{(1+\Delta m)(\omega^0_{\mathbf{k}})^2 - x\Phi^{\text{imp}}_{\mathbf{k},\mathbf{k}}}. \tag{22}$$

This is an approximated result, but physically correct: (i) If we have only an isotopic effect, then the phonon frequency is only removed, what is in agreement with other theoretical investigations [33]; (ii) Taking into account the influence of the force constants, we obtain frequency changes of the phonon modes. In dependence of the sign of the force constant changes we have hardening or softening of the mode. So, the doping contribution to the phonon energy can be written as: $\Delta\omega^{\text{imp}} = x\Phi^{\text{imp}}_{k,k}(\text{el}) + x\Phi^{\text{imp}}_{k,k}(\text{ph})$.

4 Electron Green's Function

We assume a single impurity in the graphene matrix, which substitutes a C-atom on site A in the origin of the coordinate system, and will calculate the single-site scattering matrix. We define the following Green's functions:

$$\begin{aligned}
G^{\text{imp}}_{a_n a_n}(\mathbf{k},\mathbf{q},E) &= \langle\langle a_{k,n}; a^+_{q,n}\rangle\rangle; & G^{\text{imp}}_{b_n b_n}(\mathbf{k},\mathbf{q},E) &= \langle\langle b_{k,n}; b^+_{q,n}\rangle\rangle;\\
G^{\text{imp}}_{a_n b_n}(\mathbf{k},\mathbf{q},E) &= \langle\langle a_{k,n}; b^+_{q,n}\rangle\rangle; & G^{\text{imp}}_{b_n a_n}(\mathbf{k},\mathbf{q},E) &= \langle\langle b_{k,n}; a^+_{q,n}\rangle\rangle;\\
G^{\text{imp}}_{a_{n\pm1} b_n}(\mathbf{k},\mathbf{q},E) &= \langle\langle a_{k,n\pm1}; b^+_{q,n}\rangle\rangle; & G^{\text{imp}}_{b_{n\pm1} a_n}(\mathbf{k},\mathbf{q},E) &= \langle\langle b_{k,n\pm1}; a^+_{q,n}\rangle\rangle.
\end{aligned}$$

In the next we will neglect "n". We obtain the following equation system for the Green's functions:

$$\begin{aligned}
EG^{\text{imp}}_{aa}(\mathbf{k},\mathbf{p},E) = {}& \delta_{k,p} + \sum_q \alpha_{k,q} G^{\text{imp}}_{ba}(\mathbf{q},\mathbf{p},E)\\
&+ \frac{V_k\delta_{k,0}}{N}\sum_q G^{\text{imp}}_{aa}(\mathbf{q},\mathbf{p},E) + \sum_q \beta_{k,q} G^{\text{imp}}_{aa}(\mathbf{q},\mathbf{p},E)\\
&+ \sum_q \gamma_{k,q}[G^{\text{imp}}_{b_{n+1}a}(\mathbf{q},\mathbf{p},E) + G^{\text{imp}}_{b_{n-1}a}(\mathbf{q},\mathbf{p},E)];\\
EG^{\text{imp}}_{ba}(\mathbf{k},\mathbf{p},E) = {}& \sum_q \alpha^*_{q,k} G^{\text{imp}}_{aa}(\mathbf{q},\mathbf{p},E) + \sum_q \beta^*_{q,k} G^{\text{imp}}_{ba}(\mathbf{q},\mathbf{p},E);\\
EG^{\text{imp}}_{ab}(\mathbf{k},\mathbf{p},E) = {}& \sum_q \alpha_{k,q} G^{\text{imp}}_{bb}(\mathbf{q},\mathbf{p},E) + \frac{V_k\delta_{k,0}}{N}\sum_q G^{\text{imp}}_{ab}(\mathbf{q},\mathbf{p},E)\\
&+ \sum_q \beta_{k,q} G^{\text{imp}}_{ab}(\mathbf{q},\mathbf{p},E);
\end{aligned}$$

$$EG^{\rm imp}_{bb}(\mathbf{k},\mathbf{p},E) = \delta_{k,p} + \sum_q \alpha^*_{q,k} G^{\rm imp}_{ab}(\mathbf{q},\mathbf{p},E) + \sum_q \beta^*_{q,k} G^{\rm imp}_{bb}(\mathbf{q},\mathbf{p},E)$$
$$+ \sum_q \gamma^*_{q,k}[G^{\rm imp}_{a_{n+1}b}(\mathbf{q},\mathbf{p},E) + G^{\rm imp}_{a_{n-1}b}(\mathbf{q},\mathbf{p},E)];$$
$$EG^{\rm imp}_{b_{n\pm1}a}(\mathbf{k},\mathbf{p},E) = \sum_q \beta^*_{q,k} G^{\rm imp}_{b_{n\pm1}a}(\mathbf{q},\mathbf{p},E) + \sum_q \gamma^*_{q,k} G^{\rm imp}_{aa}(\mathbf{q},\mathbf{p},E);$$
$$EG^{\rm imp}_{a_{n\pm1}b}(\mathbf{k},\mathbf{p},E) = \sum_q \beta_{k,q} G^{\rm imp}_{a_{n\pm1}b}(\mathbf{q},\mathbf{p},E) + \frac{V_k\delta_{k,0}}{N}\sum_q G^{\rm imp}_{a_{n\pm1}b}(\mathbf{q},\mathbf{p},E)$$
$$+ \sum_q \gamma_{k,q} G^{\rm imp}_{ab}(\mathbf{q},\mathbf{p},E);$$

with

$$\alpha_{k,q} = (-t_{\rm eff}\delta_{k,q} + \frac{t^{\rm imp}_{\rm eff}}{N})\sum_{\mathbf{h}_i}\exp(i\mathbf{q}.\mathbf{h}_i);$$
$$\beta_{k,q} = (-t'\delta_{k,q} + \frac{t'^{\rm imp}}{N})\sum_{\delta_i}\exp(i\mathbf{q}.\delta_i);$$
$$\gamma_{k,q} = -t_\perp\delta_{k,q} + t^{\rm imp}_\perp;$$
$$t^{\rm eff}_{ij} = t_{ij} - \frac{1}{2}\sum_r^n g_{1ijr}\langle Q_r\rangle - \frac{1}{4}\sum_{rs}^n g_{1ijrs}\langle Q_rQ_s\rangle.$$

For the impurity Green's function we obtain:

$$G^{\rm imp}_{lm}(\mathbf{k},\mathbf{p},E) \approx \delta_{k,p}G^0_{lm}(\mathbf{k},E) + G^0_{lm}(\mathbf{k},E)\tau_{lm}(E)G^0_{lm}(\mathbf{p},E), \qquad (23)$$

where $G^0_{lm}(\mathbf{k},E)$ are the Green's functions of the undoped crystal. In Eq. (23) we have neglected the terms which are proportional to the $(t^{\rm imp})^2$, i.e. they are of second order and can be neglected. For the single-site scattering matrix $\tau(E)$ we observe:

$$\tau_{lm}(E) = \frac{\Xi_{lm}(E)}{N\Lambda_{lm}(E)} \qquad (24)$$

with

$$\Xi_{lm}(E) = E[t^{\rm imp}_{\rm eff}(2t_{\rm eff} - t^{\rm imp}_{\rm eff}) + 2t^{\rm imp}_\perp(2t_\perp - t^{\rm imp}_\perp) - t'^{\rm imp}(2t' - t'^{\rm imp})]$$
$$- V_0(t^2 + t^2_\perp - t'^2) \quad \text{for} \quad l = a; \quad m = a,b; \quad \text{or}$$
$$- 0 \quad \text{for} \quad l = b; \quad m = a,b;$$
$$\Lambda_{lm}(E) = (t_{\rm eff} - t^{\rm imp}_{\rm eff})^2 + (t_\perp - t^{\rm imp}_\perp)^2 - (t' - t'^{\rm imp})^2$$
$$+ \frac{\Xi_{lm}(E)}{N}\sum_k G^0_{lm}(\mathbf{k},E), \quad l,m = a,b.$$

The scattering matrix for concentration x can be written as:

$$T_{lm}(E) = Nx\tau_{lm}(e) = x\frac{\Xi_{lm}(E)}{\Lambda_{lm}(E)}. \tag{25}$$

The Green's functions describing the properties of the doped graphene are:

$$G^{\text{imp}}_{lm}(\mathbf{k}, E) = ((G^{0}_{lm}(\mathbf{k}, E))^{-1} - T_{lm}(E))^{-1}. \tag{26}$$

From the expression:

$$\rho_{lm}(E) = \frac{1}{\pi}\text{Im}\sum_{k} G^{\text{imp}}_{lm}(\mathbf{k}, E + i\delta) \tag{27}$$

we determine the density of states function, from which the electron correlations function can be calculated as:

$$n^{\text{imp}}_{lm} = \int f_{lm}(E)\rho_{lm}(E)dE. \tag{28}$$

5 Damping

The damping is calculated using the method of Tserkovnikov [34] replacing the correlation functions for the pure graphene observed in our previous paper [30] by such due to impurity following Ferrari [35]. It is known that when impurities are induced in a pure graphene the Fermi level E_F is changed. To satisfy the Pauli principle damping is allowed only when $E_F < \hbar\omega_G/2$. This means that virtual electron-hole pair transitions with energy ranging from 0 to $2 \mid E_F \mid$ are forbidden, i.e. in this range the G-phonon decay into electron-phonon pair is forbidden. The changes in the Fermi levels in the case of low doping for SLG and BLG are respectively

$$E^{SLG}_{F}(x) = (t - t^{\text{imp}})\sqrt{\frac{\sqrt{3}\pi a}{2}n^{\text{imp}}_{SLG}(x)};$$

$$E^{BLG}_{F}(x) = -\frac{t_\perp}{2} \pm \sqrt{\frac{t^2_\perp}{2} + \frac{\sqrt{3}\pi a(t - t^{\text{imp}})^2}{2}n^{\text{imp}}_{BLG}(x)}; \quad \text{for} \quad E_F < t_\perp;$$

$$E^{BLG}_{F}(x) = (t - t^{\text{imp}})\sqrt{\frac{\sqrt{3}\pi a}{4}n^{\text{imp}}_{BLG}(x)}; \quad \text{for} \quad E_F > t_\perp.$$

For simplicity the interaction between the second neighbors is neglected.

6 Numerical Results and Discussion

From the discussion in Section 2 one can assume that the local atomic energy for carbon C is V_C = 0. Following the connection between the serial atomic

number and the atomic radius of the impurities one can differentiate two cases, p- and n-doping, for example N- and B-doping. The N atom has a smaller atomic radius than the C atom, and this corresponds to a smaller hopping amplitude between the N impurity and the neighboring and the next neighboring C atoms, i.e. t^{imp} and t'^{imp} are positive. The larger atomic number of the N atom gives a negative on-site potential with respect to the C sites, i.e. $V^{\text{imp}} < 0$ [21]. For the B atom the impurity site has larger hopping integral and a positive on-site potential, i.e. t^{imp} and t'^{imp} are negative, while $V^{\text{imp}} > 0$. Independently of the type of impurities the additive contributions to the anharmonic constants should be positive (i.e. $B^{\text{imp}} > 0$ and $A^{\text{imp}} > 0$) This is due to the violation of translation invariance which favors the process of damping and scattering of phonons. Independently of the type of impurities the G-mode hardens with increasing impurity concentration (i.e. there is a blue shift). This means that the addition term to the electron-phonon constant must be negative ($g_1^{\text{imp}} < 0$ and $g_2^{\text{imp}} < 0$). In the case of p-doping increasing of the impurity concentration leads to hardening of the 2D-mode (blue shift), whereas for the n-doping to softening of the 2D-mode (red shift). This means that for B-doping the additional terms to the electron-phonon constants are negative ($g_1^{\text{imp}} < 0$ and $g_2^{\text{imp}} < 0$), while for N-doping they are positive ($g_1^{\text{imp}} > 0$ and $g_2^{\text{imp}} > 0$). The sign of the impurity model parameters are determined on the basis of our previous papers [30,31].

We present now the numerical results of the phonon properties in ion doped graphene based on our theoretical calculations for SLG and BLG. The model parameters for the pure graphene are [30] for the G-mode: t = 2.7 eV, t' = 0.2t=0.54 eV, $t_\perp$ = 0.39 eV, g_1 = 5.3 eV/$\dot{A}$, g_2 = -4.2 eV/$\dot{A}$, ω_0 = 1582 cm^{-1}, A = -6.2 cm^{-1}, B = 2 cm^{-1}, **k** (Γ-point) - $k_x = 0$, $k_y = 0$; and for the 2D mode: t = 2.7 eV, t' = 0.54 eV, $t_\perp$ = 0.39 eV, g_1 = 10.2 eV/$\dot{A}$, g_2 = -15.5 eV/$\dot{A}$, ω_0 = 2678 cm^{-1}, A = -12.3 cm^{-1}, B = 2.7 cm^{-1}, **k**(Dirak-point) - $k_x = \frac{2\pi}{3a}, k_y = \frac{2\pi}{\sqrt{3}a}$.
In order to study the doping effects we must take into account additively the following parameters for N-doping (or B-doping), respectively: Δm = -0.1662 (0.0167); V_0 = -0.53 t (0.53 t); t^{imp} = 0.42 t (-0.53 t); t'^{imp} = 0.28 t (-0.39 t); B^{imp} = 0.28 B (0.28 B): A^{imp} = 0.28 A (0.28 A); for the G-mode: g_1^{imp} = -0.31 g_1 (-0.40 g_1); g_2^{imp} = -0.31 g_2 (-0.40 g_2); for the 2D-mode: g_1^{imp} = 0.2 g_1 (-0.26 g_1); g_2^{imp} = -0.2 g_2 (-0.26 g_2); and $m_C = 19.938 \times 10^{-27}$ kg.

The G band, related to the C-C bond stretching is the main Raman signature for all sp^2 carbons, and it is observed as a peak at around 1582 cm^{-1}. The 2D band is the second-order sp^2 Raman signature, observed for all sp^2 carbons as a peak around 2678 cm^{-1}. We consider at first the concentration dependence of the phonon G and 2D modes for different ion doping, p- or n-doping, in a SLG for T = 300 K. The results are demonstrated in Figures 2a and 2b, curves 1n (for n-doping) and 1p (for p-doping). It must be again mentioned that we consider the case of small doping concentration. The ion doped graphene shows different properties compared to the undoped graphene. In the case of p-doping (curves

(a)

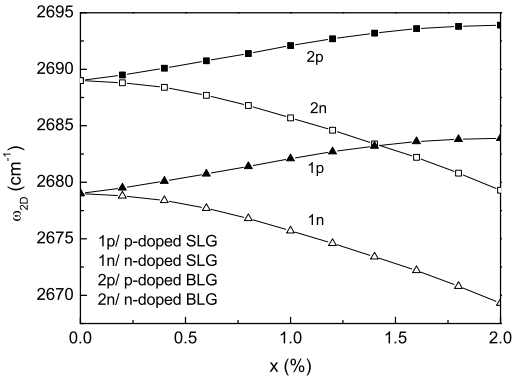

(b)

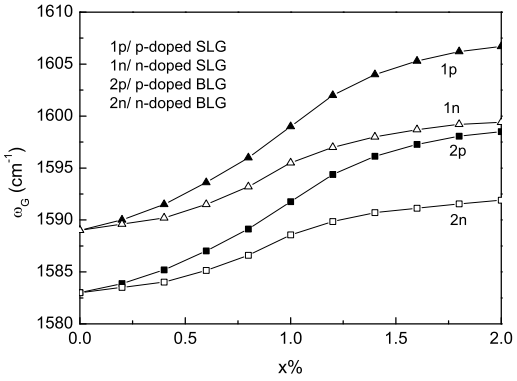

Figure 2. Doping concentration dependence of the phonon energy for (a) the 2D-mode ω_{2D} and (b) the G mode ω_G for a SLG (curves 1p and 1n) and for a BLG (curves 2p and 2n), $T = 300$ K.

1p), for example by N doping, we obtain a blue shift, an increase of the two phonon modes with increasing of the doping concentration x. This hardening of the G and 2D phonon modes is experimentally observed in N doped graphene [3-5]. Howard et al. [27] have reported that for lightly K-doped graphene the G peak hardens and narrows.

By the n-doping, for example by B doping, there are some differences in the behavior of the two phonon modes in SLG. From Figures 2a and 2b, curves 1n, can be seen that the $\omega_G(n)$ mode increases again, whereas the $\omega_{2D}(n)$ mode decreases with increasing doping concentration x. The obtained behavior is in qualitative agreement with the experimental data of Ferrari et al. [35], Das et al. [36,37], Pisana et al. [38], Jorio [39]. The significant blue or red shift of the phonon energy of the 2D mode with increasing of the doping concentration is

attributed to the interaction of the graphene with the dopants and to changes of the electronic structure, to shift of the Fermi level. In doped graphene, the shift of the Fermi energy induced by doping has two major effects: (1) a change of the equilibrium lattice parameter with a consequent stiffening/softening of the phonons, and (2) the onset of effects beyond the adiabatic Born-Oppenheimer approximation that modify the phonon dispersion close to the Kohn anomalies [38]. The excess (defect) charge results in an expansion (contraction) of the crystal lattice.

Ren et al. [40] have studied the doping effect of metals on graphene. The results show that Ag and Cu cause a shift in the Fermi level in the graphene from the Dirac point into the conduction band while Au causes a shift into the valence band. The shifts in the Fermi level of the graphene are explained by the different work functions of these metals. Iqbal et al. [41] have shown using Raman spectroscopy that the properties of SLG are strongly affected by metal doping. The shifts in G and 2D peak positions indicate the doping effect of graphene by Cr and Ti metals. While p-type doping was observed for Cr-coated graphene, n-type doping was observed for Ti-coated graphene.

In Figures 2a and 2b we have discussed the concentration dependence of the phonon modes. But the position of the peaks is also changed due to the electron-phonon interaction. As the electronic structure is modified, so too is the electron-phonon interaction. Since this interaction plays an important role in the dynamics of charge carriers, understanding its effects in SLG and BLG is of crucial importance for graphene-based electronics [27]. The effect of the electron-phonon interaction on the phonon shifts of the p- or n-doped 2D modes in a SLG is shown in the next Figures 3a and 3b. It can be seen that in the two Figures the electron-phonon contribution increases (curve 1), whereas that of the phonon-phonon interaction decreases (curve 3) with increasing of doping concentration x. But there are some differences in the behavior of the p- and n-doped modes. The changes in the p-doped SLG due to the electron-phonon interaction are larger than those from the phonon-phonon interaction, so that finally the 2D mode increases with x (Figure 3a). The n-doped SLG shows the opposite behavior to that of the p-doped SLG. The changes due to the electron-phonon interaction are smaller compared to those from the phonon-phonon interaction, so that finally the phonon shift of the 2D mode decreases with x (Figure 3b). The contribution of the different interaction mechanisms, electron-phonon and phonon-phonon interactions, in the concentration dependence of the phonon shift of the p- or n-doped G mode is analogously to those shown in Fig. 3a, i.e. to the p-doped ω_{2D} mode. At light doping levels a small hardening in the in-plane carbon phonon energies and narrowing in their line-width have been reported for the G mode [38]. This is due to a reduction in the electron-phonon scattering as the Kohn anomaly found in pure graphene at Γ is gradually removed to finite $\mathbf{q}$. Higher doping levels can cause blue (red) shift for p (n) doping in the G mode [39].

(a)

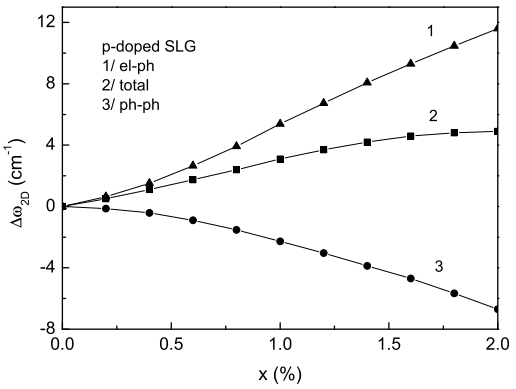

(b)

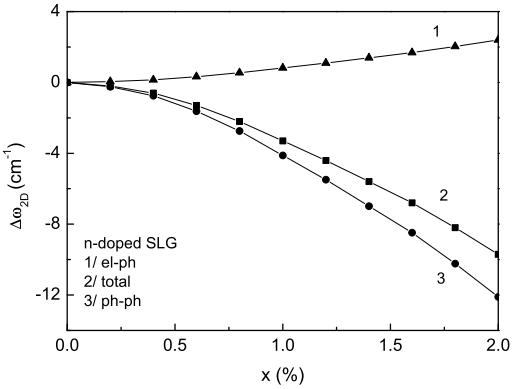

Figure 3. Doping concentration dependence of the phonon energy shift for the (a) p-doped and (b) n-doped 2D-mode $\Delta\omega_{2D}$ for a SLG, T = 300 K, where (1) contribution from the electron-phonon interaction, (2) total phonon shift, (3) contribution from the phonon-phonon interaction.

The damping of the G and 2D mode (Γ_G and Γ_{2D}) in a p- or n-doped SLG which corresponds to the full width at half maximum (FWHM) of the Raman peaks is also different compared to the pure case. It increases with increasing ion doping concentration for the 2D mode, whereas for the G mode it decreases (Figures 4a and 4b, curves 1p and 1n). This is in agreement with the experimental data [27,37]. Reduction of the half-width of the G-mode due to the blocking of the phonon damping in electron-hole pairs which is a consequence of the principle of Pauli. The FWHM(G) decreases for both electron and hole doping, as expected since phonons decay into real electron-hole pairs when $E_F < \hbar\omega_0/2$. The decrease in line-width saturates when the doping causes a Fermi-level shift bigger than half the phonon energy [38].

(a)

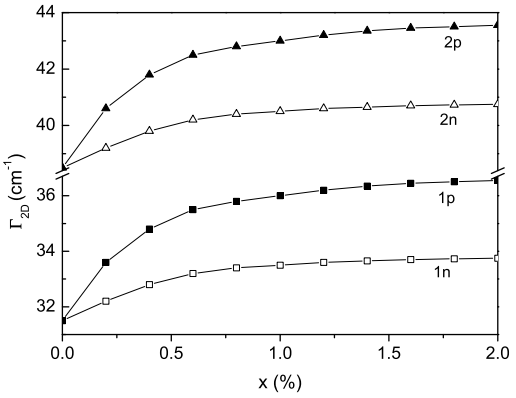

(b)

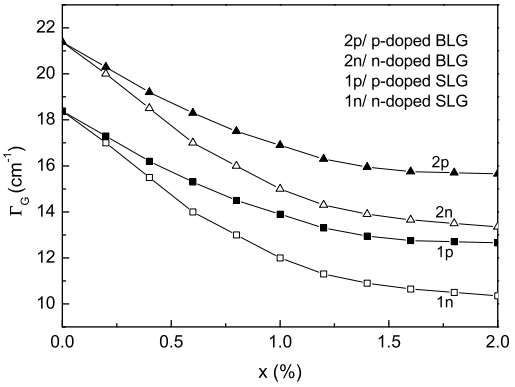

Figure 4. Doping concentration dependence of the phonon damping for (a) the 2D-mode Γ_{2D} and (b) the G mode Γ_G for a SLG (curves 1p and 1n) and for a BLG (curves 2p and 2n), T = 300 K.

The electron-phonon interaction influences also the phonon damping of the p- and n-doped SLG. This is demonstrated in Figures 5a and 5b. The line-width for the G peak is usually in the range of 10-15 cm^{-1} [39], what is in agreement with our results (Figure 5b), although it changes with strain, temperature, and doping. It can be seen from the two Figures that in the case of p-doping $\Gamma_{2D}(p)$ increases, whereas $\Gamma_G(p)$ decreases with increasing concentration x. This is due to the different interaction mechanisms. The contribution of the electron-phonon and phonon-phonon interactions is complicated compared to that of the phonon energies, it is changed for small and larger concentrations. In the case of p-doped SLG the electron-phonon interaction causes an increase of Γ_{2D}, whereas the phonon-phonon interaction – a decrease. For small x val-

(a)

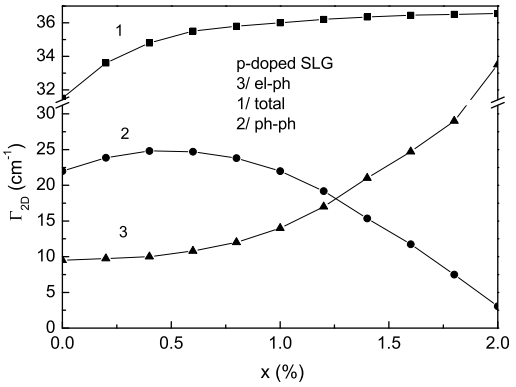

(b)

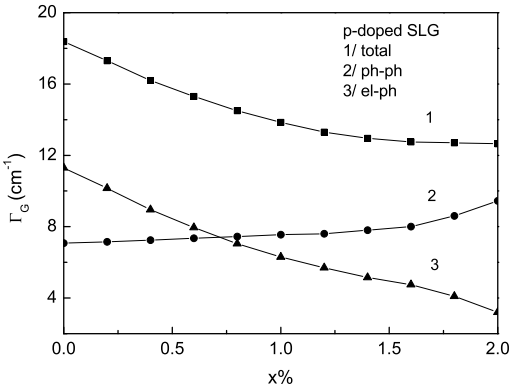

Figure 5. Doping concentration dependence of the phonon damping for the p-doped (a) 2D mode Γ_{2D} and (b) G-mode Γ_G for a SLG, T = 300 K, where (1) total, (2) contribution from the phonon-phonon interaction, (3) contribution from the electron-phonon interaction.

ues ($< 1.25\%$) the contribution from the phonon-phonon interaction is larger, whereas for $x > 1.25\%$ the electron-phonon interaction is larger and leads to the saturation value of $\Gamma_{2D}(p)$ in p-doped SLG. The behavior of $\Gamma_{2D}(n)$ is similarly to that of $\Gamma_{2D}(p)$.

In the case of p-doping the contribution of the different interaction mechanisms in the damping of the G mode, $\Gamma_G(p)$, is opposite to that of $\Gamma_{2d}(p)$, i.e. the electron-phonon interaction causes a decrease, whereas the phonon-phonon interaction – an increase of $\Gamma_G(p)$. The contribution from the electron-phonon interaction is again larger compared to that of the phonon-phonon interaction, so that finally Γ_G decreases with increasing doping concentration x. The $\Gamma_G(n)$ dependence of the electron-phonon interaction is analogously to the of $\Gamma_G(p)$.

In order to further explore the effect of dimensionality, we have studied doped SLG and BLG. The conceptually different BLG band structure is expected to renormalize the phonon response to doping differently from SLG. Here we prove this by investigating the effect of doping on the G and 2D peaks in a BLG, taking into account the interlayer interactions $t_\perp$. It can be seen from Figures 2a and 2b, curves 2p and 2n, that the concentration dependence of p- or n-doped BLG is the same as of SLG, ω_{2D} can increase or decrease, whereas ω_G only increases. But ω_{2D} is larger in BLG compared to that of SLG, whereas ω_G is smaller in BLG than SLG, i.e. ω_{2D} is increased in BLG, whereas ω_G is decreased.

The dependence of Γ_{2D} and Γ_G on the dimensionality is also calculated and shown in Figures 4a and 4b (curves 2p and 2n). It can be seen that the damping of the two phonon modes in BLG is increased compared to the SLG, what is in agreement with the experimental data of Das et al. [37]. The dependence of the phonon damping for the two modes on the layer thickness of graphene is in agreement with the results observed from pure graphene in our previous paper [30].

7 Conclusions

Using a microscopic model we have shown that the phonon spectra of the G and 2D modes near Γ and K points of the Brillouin zone are strongly affected by p- or n-doping. It is shown that the G and 2D modes in a SLG have different doping dependence. Doping upshifts and sharpens the G peak for both holes and electrons, whereas the 2D peak shows hardening or softening for p- or n-doping and broadening for both doping types. The electron-phonon interaction and their contribution compared to the phonon-phonon interaction in the phonon spectrum is discussed. Finally we have calculated and discussed the phonon properties in a BLG. There is a good agreement with the experimental data. In conclusion, this work offers an insight into the defect-activated phonon process, which will be useful to improve our understanding and modelling of defects in graphene.

References

[1] Y.A. Kim, K. Fujisawa, H. Muramatsu, T. Hayashi, M. Endo, T. Fujimori, K. Kaneko, M. Terrones, J. Behrends, A. Eckmann, C. Casiraghi, K.S. Novoselov, R. Saito, M.S. Dresselhaus (2012) *ACS Nano* **6** 6293.

[2] R. Lv, M. Terrones (2012) *Mater. Lett.* **78** 209.

[3] B. Guo, Q. Liu, E. Chen, H. Zhu, L. Fang, J.R. Gong (2010) *Nano Lett*. **10** 4975.

[4] R. Yang, Q.S. Huang, X.L. Chen, G.Y. Zhang, H.-J. Gao (2010) *J. Appl. Phys.* **107** 034305.

[5] H. Wang, T. Maiyalagan, X. Wang (2012) *ACS Catal.* **2** 781.

[6] L. Ci, L. Song, C. Jin, D. Jariwala, D. Wu, Y. Li, A. Srivastava, Z.F. Wang, K. Storr, L. Balicas, F. Liu, P.M. Ajayan (2010) *Nat. Mater*. **9** 430.

[7] T.B. Martins, R.H. Miwa, A.J.R. da Silva, A. Fazzio (2007) *Phys. Rev. Lett*. **98** 196803.
[8] S. Yu, W. Zheng, C. Wang, Q. Jiang (2010) *ACS Nano* **4** 7619.
[9] E.J.G. Santos, A. Ayuela, D. Sanchez-Portal (2012) *J. Phys. Chem. C* **116** 1174.
[10] M. Wu, C. Cao, J.Z. Jiang (2010) *New J. Phys.* **12** 063020.
[11] K. Pi, K.M. McCreary, W. Bao, W. Han, Y.F. Chiang, Y. Li, S.-W. Tsai, C.N. Lau, R.K. Kawakami (2009) *Phys. Rev. B* **80** 075406.
[12] T. Elbo, M. Wasniowska, P. Thakur, M. Gyamfi, B. Sachs, T.O. Wehling, S. Forti, U. Starke, C. Tieg, A.I. Lichtenstein, R. Wiesendanger (2013) *Phys. Rev. Lett.* **110** 136804.
[13] F.M. Hu, T. Ma, H.-Q. Lin, J.E. Gubernatis (2011) *Phys. Rev. B* **84** 075414.
[14] J.E. Santos, N.M.R. Peres, J.M.B. Lopes dos Santos, A.H.C. Neto (2011) *Phys. Rev. B* **84** 085430.
[15] C.D. Porter, D. Stroud (2012) *Phys. Rev. B* **85** 235452.
[16] L.S. Panchakarla, K.S. Subrahmanyam, S.K. Saha, A. Govindaraj, H.R. Krishnamurthy, U.V. Waghmare, C.N.R. Rao (2009) *Adv. Mater.* **21** 4726.
[17] S. Mukherjee, T.P. Kaloni (2012) *J. Nanopart. Res.* **14** 1059.
[18] M.K. Srivastava, Y. Wang, A.F. Kemper, H.-P. Cheng (2012) *Phys. Rev. B* **85** 165444.
[19] M. Wu, C. Cao, J.Z. Jiang (2010) *Nanotechnology* **21** 505202.
[20] K.T. Chan, J.B. Neaton, M.L. Cohen (2008) *Phys. Rev. B* **77** 235430.
[21] T.G. Pedersen, J.G. Pedersen (2013) *Phys. Rev. B* **87** 155433.
[22] C. Casiraghi (2009) *Phys. Rev. B* **80** 233407.
[23] S.K. Gupta, H.R. Soni, P.K. Jha (2013) *AIP Adv.* **3** 032117.
[24] H. Sahin, S. Ciraci (2012) *J. Phys. Chem. C* **116** 24075.
[25] D.M. Basko, S. Piscanec, A.C. Ferrari (2009) *Phys. Rev. B* **80** 165413.
[26] N. Jung, B. Kim, A.C. Crowther, N. Kim, C. Nuckolls, L. Brus (2011) *ACS Nano* **5** 5708.
[27] C.A. Howard, M.P.M. Dean, F. Withers (2011) *Phys. Rev. B* **84** 241404(R).
[28] D. Abdula, K.T. Nguyen, K. Kang, S. Fong, T. Ozel, D.G. Cahill, M. Shim (2011) *Phys. Rev. B* **83** 205419.
[29] D. Choudhury, B. Das, D.D. Sarma, C.N.R. Rao (2010) *Chem. Phys. Lett.* **497** 66.
[30] A.T. Apostolov, I.N. Apostolova, J.M. Wesselinowa (2012) *J. Phys.: Condens. Matter* **24** 235401.
[31] A.T. Apostolov, I.N. Apostolova, J.M. Wesselinowa (2012) *Solid State Commun.* **152** 1980.
[32] R.W. Davies, J.S. Langer (1963) *Phys. Rev.* **131** 163.
[33] R.J. Elliott, J.A. Krumhansel, P.L. Leath (1974) *Rev. Mod. Phys*. **46** 465.
[34] Yu. A. Tserkovnikov (1971) *Teor. Mat. Fiz.* **7** 250.
[35] A.C. Ferrari (2007) *Solid State Commun.* **143** 47.
[36] A. Das, S. Pisana, B. Chakraborty, S. Piscanec, S.K. Saha, U.V. Waghmare, K.S. Novoselov, H.R. Krishnamurthy, A.K. Geim, A.C. Ferrari, A.K. Sood (2008) *Nanotechnology* **3** 210.
[37] A. Das, B. Chakraborty, S. Piscanec, S. Pisana, A.K. Sood, A.C. Ferrari (2009) *Phys. Rev. B* **79** 155417.

[38] S. Pisana, M. Lazzeri, C. Casiraghi, K.S. Novoselov, A.K. Geim, A.C. Ferrari, F. Mauri (2007) *Nat. Mater.* **6** 198.

[39] A. Jorio (2012) *ISRN Nanotechno;ogu* **2012** 1.

[40] Y. Ren, S. Chen, W. Cai, Y. Zhu, C. Zhu, R.S. Ruoff (2010) *Appl. Phys. Lett*. **97** 053107.

[41] M.W. Iqbal, A.K. Singh, M.Z. Iqbal, J. Eom (2012) *J. Phys.: Condens. Matter* **24** 335301.